

# Reaction Pathways of Singlet Silylene and Singlet Germylene with Water, Methanol, Ethanol, Dimethyl Ether, and Trifluoromethanol: An *ab Initio* Molecular Orbital Study

Michael W. Heaven, Gregory F. Metha, and Mark. A. Buntine\*

Department of Chemistry, University of Adelaide, Adelaide, SA 5005 Australia

Received: August 8, 2000; In Final Form: November 28, 2000

*Ab initio* molecular orbital calculations have been performed to explore the reaction potential energy surfaces of singlet silylene and germylene with water, methanol, ethanol, dimethyl ether, and trifluoromethanol. We have identified two new reaction channels on each reaction surface, except for reactions involving dimethyl ether. The previously unreported reaction channels involve H<sub>2</sub> elimination following the initial formation of an association complex. For reactions involving singlet silylene and water, a simple activated complex theory (ACT) analysis predicts that these newly identified reaction channels are equally likely to be accessed as the previously identified 1,2 hydrogen atom shift channels. For reactions involving singlet germylene and water, a similar ACT analysis predicts that the H<sub>2</sub>-elimination channels will occur in preference to the 1,2 hydrogen shift. Indeed, the room-temperature rate constants for H<sub>2</sub> elimination from the germanium complex are predicted to be approximately 5 orders of magnitude greater than for the H atom migration channel.

## 1. Introduction

The chemistry of silylene, SiH<sub>2</sub>, and to a lesser extent germylene, GeH<sub>2</sub>, has been the focus of a considerable amount of attention over the last 2 decades due to the importance of these group IV electron-deficient radicals in chemical vapor deposition, semiconductor manufacture, and the photonics and aerospace industries.<sup>1–4</sup> In particular, the oxidation chemistry of silylene has received considerable attention, both experimental and theoretical, in recent years.<sup>5,6</sup> For example, silylene is well-known to insert into O–H bonds<sup>7,8</sup> via a zwitterionic donor–acceptor intermediate.<sup>9</sup> Nonetheless, there remains a paucity of experimental data characterizing the energetics and kinetics of silylene oxidation chemistry. Even less experimental data are available to characterize the oxidation chemistry of germylene.

*Ab initio* quantum chemistry has proven to be a valuable tool in developing a more detailed understanding of the chemistry of the silicon-oxy-hydrides, Si<sub>x</sub>H<sub>y</sub>O<sub>z</sub>. The first theoretical study of silylene insertion into O–H bonds was made by Raghavachari et al. in 1984.<sup>10</sup> Gordon and Pederson<sup>5</sup> studied the reverse reaction in 1990 as part of an investigation into thermal decomposition processes for silanol. More accurate calculations describing the insertion of silylene into water were reported by Su and Gordon in 1993,<sup>11</sup> while in the same year Darling and Schlegel<sup>12</sup> and Lucas et al.<sup>13</sup> reported extensive tabulations of thermochemical data for the SiH<sub>x</sub>O<sub>y</sub> system using the G-2<sup>14</sup> method. Accurate thermochemical data for the Si<sub>x</sub>H<sub>y</sub>O<sub>z</sub> system were reported by Zachariah and Tsang in 1995.<sup>6</sup> In 1996, Lee and Boo<sup>15</sup> investigated the propensity for silylene insertion into CH<sub>3</sub>O–H and CH<sub>3</sub>–OH via *ab initio* theory. There are no reports in the literature describing the results of similar theoretical investigations into the oxidation chemistry of germylene.

In an effort to gain a more detailed understanding of the oxidation chemistry of silylene and germylene, Alexander et

al. have measured the removal rate constants for singlet silylene and germylene reacting with dimethyl ether, methanol, water, and related compounds.<sup>16</sup> In particular, a motivation for measuring the pressure-independent removal rate constants has been to provide reliable experimental data to be used in subsequent reaction modeling. Nonetheless, without a more detailed knowledge of the relevant reaction potential energy surfaces, interpretation of the experimental data can be difficult. It is therefore desirable to extend the already extensive body of theoretical literature describing the silylene-plus-water system by making an investigation into the reactivity of singlet silylene and germylene with other compounds of experimental interest.

This paper presents the results of a new theoretical investigation into the reaction pathways of silylene with water, methanol, ethanol, dimethyl ether, and trifluoromethanol. In addition, in light of the lack of theoretical data on the analogous germylene systems, we report the first *ab initio* results describing the oxidation chemistry of germylene with water and methanol. We have identified new reaction channels on the silylene-alcohol and germylene-alcohol reaction potential energy surfaces. This new computational study provides fresh insight into the relevant oxidation chemistry of silylene and germylene, predicting that H<sub>2</sub> elimination is an important reaction channel for both systems at lower reaction temperatures than previously anticipated.

## 2. Computational Details

The computational approach we have adopted for this study is broadly similar to that previously reported by Su and Gordon in their study of the insertion of silylene and dimethylsilylene into water.<sup>11</sup>

All calculations were performed using the Gaussian 94<sup>17</sup> and Gaussian 98<sup>18</sup> suites of programs. Geometry optimizations were performed using the Pople-type 6-311++G(d,p) basis set. This flexible triple- $\zeta$  basis set was chosen because (i) it allows for a direct comparison of the reaction potential energy surfaces involving the silicon and germanium analogues, and (ii) it reproduces the pertinent features of the silylene-plus-water

\* To whom correspondence should be addressed. Address: Department of Chemistry, University of Adelaide, Adelaide, SA 5005, Australia. Fax: +61-8-8303-4358. E-mail: mark.buntine@adelaide.edu.au.

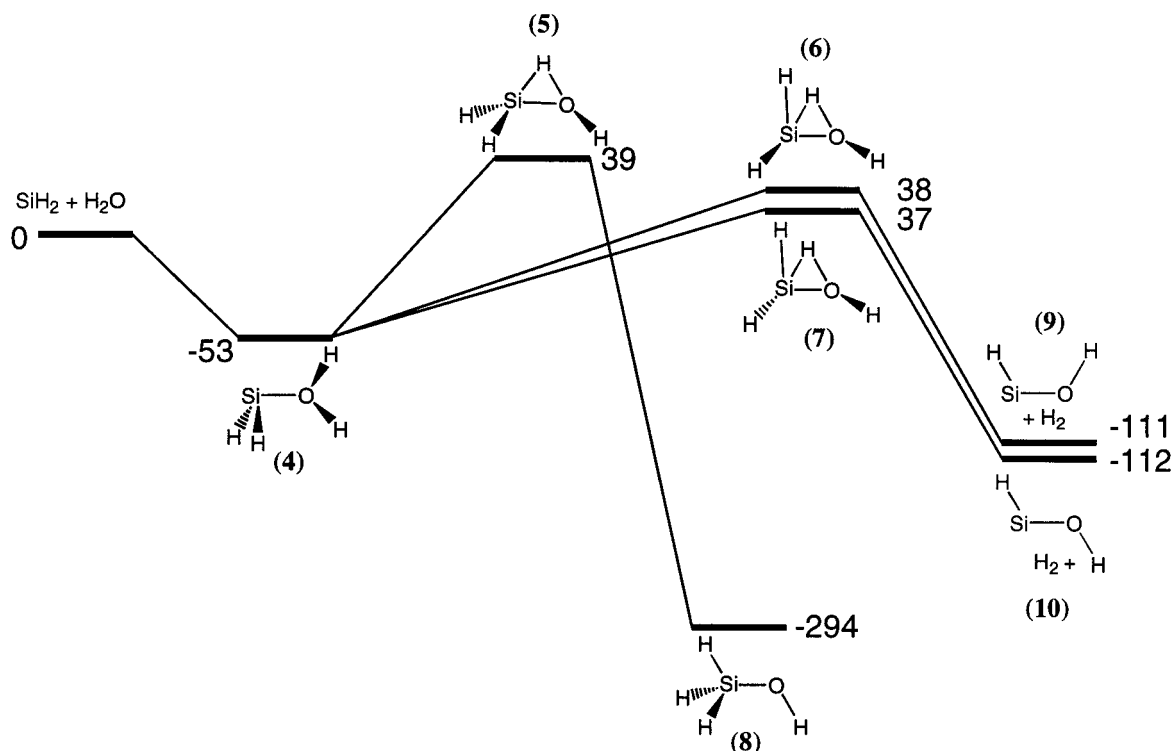


**Figure 1.** MP2/6-311++G(d,p) stationary points determined on the silylene-plus-water reaction potential energy surface. Note that the pathways leading to the formation of *syn*- **9** and *anti*-hydroxysilylene **10** via transition states **6** and **7**, respectively, are hitherto unknown.

**TABLE 1: Number of Molecular Orbitals Included in the Frozen Core for Each Post-HF *ab Initio* Calculation**

reaction system	number of orbitals in frozen core
SiH <sub>2</sub> + H <sub>2</sub> O	6
SiH <sub>2</sub> + MeOH	7
SiH <sub>2</sub> + EtOH	8
SiH <sub>2</sub> + CF <sub>3</sub> OH	10
SiH <sub>2</sub> + MeOMe	8
GeH <sub>2</sub> + H <sub>2</sub> O	15
GeH <sub>2</sub> + MeOH	16
GeH <sub>2</sub> + MeOMe	17

reaction potential energy surface as previously reported in the literature.<sup>1,5,10–12</sup>

The geometries of all stationary points on the reaction potential energy surfaces were first determined at the Hartree–Fock (HF) level of theory and then reoptimized using second-order Møller–Plesset perturbation theory (MP2). For the silylene-plus-water reaction system more extensive optimizations were performed at the MP4(SDTQ)<sup>19,20</sup> and QCISD(T)<sup>21,22</sup> levels of theory. All MP2, MP4(SDTQ), and QCISD(T) calculations were performed with a frozen core of inner electrons. That is, only the valence electrons and virtual orbitals were used in the electron correlation calculations. The number of molecular orbitals constrained to the frozen core for each reaction system is listed in Table 1.

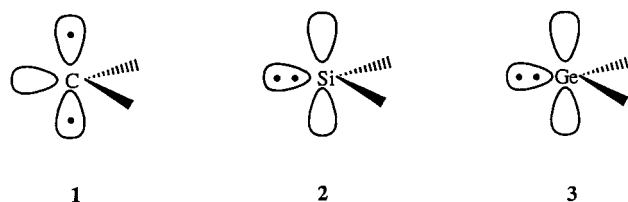
Stationary points on each reaction potential energy surface were characterized as being minima or transition states by diagonalizing the second-derivative Hessian matrix to determine the number of negative eigenvalues (0 for minima, 1 for transition states).<sup>23</sup> All reported zero-point energies are scaled by 0.8929.<sup>22,24</sup>

To verify that transition states identified by the computational procedure described above actually connect to the expected reactants, intermediates and products for each reaction channel, intrinsic reaction coordinate (IRC)<sup>25</sup> calculations were per-

formed, in which the paths of steepest descent (in mass-weighted Cartesian coordinates) were followed from each transition state to the connecting minima. The default step size along the reaction path was 0.1 amu<sup>1/2</sup> bohr.

### 3. Results and Discussion

Unlike carbene, CH<sub>2</sub> (**1**), which exists in its ground electronic state as a triplet with unpaired valence electrons, silylene, SiH<sub>2</sub> (**2**), and germylene, GeH<sub>2</sub> (**3**), exhibit vastly different chemistry due to the pairing of the valence electrons to create singlet ground electronic states. The pairing of the valence electrons creates empty p atomic-like molecular orbitals at the silicon and germanium atomic centers that are available to accept electron density from electron-rich reaction partners. In this study we explore the reactivity of singlet silylene and germylene with small electron-rich alcohols and related compounds. In the sections below we present the results for, and discuss the reaction potential energy surfaces of, each sub-titled reaction.



**3.1. SiH<sub>2</sub> + H<sub>2</sub>O.** The insertion reaction of silylene into water is the most thoroughly investigated of all the reactions considered here and was first studied by Raghavachari et al.,<sup>10</sup> with subsequent investigations by Gordon and Pederson<sup>5</sup> and Su and Gordon.<sup>11</sup> Related chemistry has been investigated by Darling and Schlegel,<sup>12</sup> Lucas et al.,<sup>13</sup> and Zachariah and Tsang.<sup>1</sup> Together, this body of work has provided a detailed picture of much of the silicon-oxy-hydride potential energy surface. A pictorial summary of the reaction profiles determined from our

**TABLE 2: Molecular Point Group Symmetry, Total Energy, Scaled Zero-Point Energy (ZPE), Hessian Index, and Selected Geometric Parameters for Each Stationary Point on the Silylene-plus-Water Reaction Potential Energy Surface<sup>a</sup>**

	total energy	ZPE	Hessian index	$r(\text{Si}-\text{O})$	$r(\text{O}-\text{H}_c)$	$r(\text{Si}-\text{H}_c)$	$\angle(\text{Si}-\text{O}-\text{H}_d)$	$\angle(\text{Si}-\text{O}-\text{H}_c)$	$\angle(\text{H}_a-\text{Si}-\text{H}_b)$
reactants (SiH <sub>2</sub> + H <sub>2</sub> O)			0						
HF	-366.07706	83.2			0.94				93.7
MP2	-366.38654	79.5			0.96				92.5
MP4(SDTQ)	-366.42428	78.7			0.96				92.3
QCISD(T)	-366.42689	78.6			0.96				92.6
intermediate complex (4)			0						
HF	-366.09639	97.5		2.15	0.94	2.72	120.5	117.9	95.0
MP2	-366.41249	94.3		2.12	0.96	2.67	117.1	115.0	94.3
MP4(SDTQ)	-366.44923	93.4		2.14	0.96	2.69	116.0	115.4	94.1
QCISD(T)	-366.45093	93.2		2.14	0.96	2.70	116.4	115.3	94.2
transition state (5)			1						
HF	-366.03297	86.5		1.86	1.25	1.62	122.2	59.0	105.0
MP2	-366.37299	82.4		1.95	1.26	1.62	112.7	55.9	104.7
MP4(SDTQ)	-366.40868	81.3		1.97	1.27	1.62	111.5	55.2	104.6
QCISD(T)	-366.40856	81.5		1.95	1.27	1.62	112.8	55.8	104.8
transition state (6)			1						
HF	-366.03813	88.5		1.87	1.26	1.76	120.0	65.4	89.2
MP2	-366.37393	84.7		1.91	1.30	1.75	115.6	62.8	87.8
MP4(SDTQ)	-366.41026	83.6		1.92	1.31	1.76	115.2	62.7	87.7
QCISD(T)	-366.41062	83.6		1.91	1.30	1.76	115.7	63.0	87.7
transition state (7)			1						
HF	-366.03893	89.2		1.87	1.26	1.77	116.9	65.6	89.6
MP2	-366.37482	85.6		1.91	1.29	1.76	112.4	63.1	88.5
MP4(SDTQ)	-366.41112	84.5		1.92	1.30	1.76	112.1	62.9	88.5
QCISD(T)	-366.41142	84.5		1.91	1.30	1.76	112.6	63.2	88.4
silanol (8)			0						
HF	-366.18812	95.8		1.64	2.50	1.47	122.6	34.3	108.1
MP2	-366.50366	92.7		1.67	2.50	1.47	118.4	34.4	108.0
MP4(SDTQ)	-366.53661	91.9		1.67	2.51	1.47	117.7	34.4	108.0
QCISD(T)	-366.53705	91.8		1.67	2.51	1.47	117.9	34.4	108.0
syn-hydroxysilylene (9)			0						
HF	-364.97540	51.4		1.64			123.7		
MP2	-365.26623	49.0		1.67			119.4		
MP4(SDTQ)	-365.29552	48.5		1.68			118.9		
QCISD(T)	-365.29627	48.5		1.67			119.3		
anti-hydroxysilylene (10)			0						
HF	-364.97536	52.1		1.64			118.7		
MP2	-365.26686	49.8		1.68			113.9		
MP4(SDTQ)	-365.29615	49.3		1.68			113.7		
QCISD(T)	-365.29677	49.3		1.68			114.2		
hydrogen (H <sub>2</sub> )			0						
HF	-1.13251	24.5							
MP2	-1.16030	24.2							
MP4(SDTQ)	-1.16777	23.8							
QCISD(T)	-1.16838	23.6							

<sup>a</sup> Results are reported using the Pople-type 6-311++G(d,p) basis set at the HF, MP2, MP4(SDTQ), and QCISD(T) levels of theory. The point group and Hessian index results apply for all the levels of theory. Total energies are in hartrees. ZPEs are in kJ/mol. Distances are in angstroms. Angles are in degrees. Geometric parameters without listed values have no meaning in the atom labeling scheme employed.

MP2/6-311++G(d,p) investigation is presented in Figure 1.<sup>26</sup> We have identified two new reaction channels leading to the formation of syn- and anti-hydroxysilylene from the reaction of silylene and water. These newly identified reaction channels suggest that the onset of H<sub>2</sub> elimination may occur at excitation energies (and hence reaction temperatures) lower than previously thought.<sup>1</sup> Note that it is the pathways leading to the formation of syn- and anti-hydroxysilylene, structures **9** and **10**, respectively, via transition states **6** and **7**, respectively, that are reported here for the first time.

In Table 2 we report the point group symmetry of each geometry-optimized stationary point on the silylene-plus-water reaction surface, as well as the total energy, scaled zero-point

energy, Hessian index and selected geometric parameters for each stationary point. Results are reported for Hartree-Fock (HF) theory, second-order Møller-Plesset perturbation (MP2) theory, fourth-order Møller-Plesset perturbation (MP4(SDTQ)) theory<sup>19</sup> and quadratic configuration interaction (QCISD(T)) theory.<sup>21</sup> The reported subset of geometric parameters represent the critical bond-forming, bond-breaking and geometry-changing degrees of freedom along the reaction pathways. A complete listing of all structural information and calculated (unscaled) vibrational frequencies for each stationary point, at each level of theory, is available as supplementary information.<sup>27</sup>

From Table 2 it is apparent that, for each level of theory, the calculated stationary point geometries do not vary significantly

**TABLE 3: Comparison of the Relative Energies of Stationary Points on the Silylene-plus-Water Reaction Potential Energy Surface as Determined in This Study<sup>a,b</sup> and in Previous Investigations<sup>c-e</sup>**

	$\Delta E(\text{HF})^b$	$\Delta E(\text{MP2})^b$	$\Delta E(\text{MP4})^b$	$\Delta E(\text{QCISD(T)})^b$	$\Delta E(\text{Rag.})^c$	$\Delta E(\text{Su})^d$	$\Delta E(\text{Zac.})^e$
intermediate complex ( <b>4</b> )	-36.5	-53.3	-50.8	-48.5	-55.6	-86.2	-36.2
transition state ( <b>5</b> )	119.1	38.5	43.6	51.0	36.4	20.5	13.1
transition state ( <b>6</b> )	107.5	38.3	41.7	47.8			
transition state ( <b>7</b> )	106.2	36.9	40.3	46.5			
silanol ( <b>8</b> )	-278.9	-294.3	-281.7	-276.1	-293.7	-320.1	-317.9
<i>syn</i> -hydroxysilylene ( <b>9</b> ) + hydrogen	-88.2	-111.3	-108.9	-105.6			
<i>anti</i> -hydroxysilylene ( <b>10</b> ) + hydrogen	-87.4	-112.1	-109.7	-106.1			-127.7

<sup>a</sup> All values are reported in kJ/mol. Note the trend for the work performed in this study where the post-HF relative energies for each stationary point increase in the order MP2:MP4(SDTQ):QCISD(T). See text for details. <sup>b</sup> All calculations in this study were performed with the 6-311++G(d,p) basis set at the four levels of theory specified. <sup>c</sup> Work of Raghavachari et al. (ref 10) at the HF/6-31G(d) level. <sup>d</sup> Work of Su and Gordon (ref 11) at the MP2/6-31G(d,p) level. <sup>e</sup> Work of Zachariah and Tsang (ref 4) at the MP4/6-311G(2df, p)/MP2/6-31G(d) level.

from each other, particularly for the post-Hartree–Fock calculations. However, the level of theory employed does show a significant variation in the predicted total energy of each stationary point. In particular, the introduction of electron correlation in the post-Hartree–Fock calculations has a large effect on the predicted energies. The influence of the level of theory employed on the predicted energies of the stationary points can be seen more clearly in Table 3 where we report the relative energies, including scaled zero-point energies, of all stationary points on the reaction surface, determined both in this study at all four levels of theory and, where available, by previous investigators.<sup>1,10,11</sup>

The MP4 calculations predict a *decrease* in the well depth for intermediate **4** of 2.5 kJ/mol and an *increase* in the barrier height for transition state **5** by 5.1 kJ/mol, relative to the MP2 energy predictions. Similarly, relative to the MP4(SDTQ) results, the QCISD(T) calculations predict a *further decrease* in the well depth for intermediate **4** of 2.3 kJ/mol and a *further increase* in the barrier height for transition state **5** of 7.4 kJ/mol. Indeed, the data in Table 3 clearly show a consistent trend wherein the relative energies of all local minima on the reaction potential energy surface *decrease* as the level of theory employed moves from MP2 to MP4(SDTQ) to QCISD(T), while the relative energies of all transition states *increase* as the level of theory is improved. These trends are similar to those reported by Su and Gordon<sup>11</sup> where energy variations of 2–8 kJ/mol were observed as the level of theory was improved. Su and Gordon performed high level single-point energy corrections to the optimized MP2 geometries, whereas in this study full optimizations were performed at each level of theory (albeit with a frozen core treatment for electron correlation). Nonetheless, the consistent trends of increasing and decreasing relative energies for each stationary point as a function of improving the level of theory indicates that it is sufficient to limit our calculations to the less computationally expensive MP2 level for all further reactions studied here. Reasonable estimates of well depths and reaction barriers for the higher levels of theory can be made, if necessary, by simply adding or subtracting (as appropriate) 2–7 kJ/mol to the reported MP2 results.

The silylene-plus-water reaction is initiated by an interaction between the empty p atomic-like orbital on the ground-state SiH<sub>2</sub> and a lone pair of electrons on the water, leading to intermediate **4** possessing C<sub>1</sub> symmetry and bound by 53.3 kJ/mol at the MP2 level<sup>26</sup> (cf. 55.6 kJ/mol predicted by Raghavachari et al.<sup>10</sup> using HF/6-31G(d) and 86.2 kJ/mol predicted by Su et al.<sup>11</sup> using MP2/6-31G(d,p)). The interaction binding intermediate **4** results in the plane of the SiH<sub>2</sub> moiety lying almost orthogonal to the Si–O axis. The Si–O bond length is long, calculated to be 2.12 Å, compared to 2.13 Å predicted by Raghavachari et al.<sup>10</sup> and 2.10 Å predicted by Su et al.<sup>11</sup>

Rearrangement of intermediate **4** to silanol **8** (see Figure 1) has been previously shown to proceed via transition state **5** (involving a 1,2 hydrogen shift), a stationary point on the reaction potential energy surface identified to possess C<sub>1</sub> symmetry.<sup>10</sup> We calculate the Si–O bond length in transition state **5** to be 1.95 Å, compared to 1.87 Å predicted by Raghavachari et al.<sup>10</sup> and 1.93 Å predicted by Su and Gordon.<sup>11</sup> The net activation barrier for the formation of silanol is calculated by us to be 38.5 kJ/mol, compared to 36.4 kJ/mol by Raghavachari et al.<sup>10</sup> and 20.5 kJ/mol by Su and Gordon.<sup>11</sup> Moreover, we calculate that the overall energy barrier from intermediate **4** to transition state **5** is 91.8 kJ/mol, compared to 92.0 kJ/mol predicted by Raghavachari et al.<sup>10</sup> and 106.7 kJ/mol by Su and Gordon.<sup>11</sup> Finally, the formation of silanol **8** from silylene and water is calculated by us to be exothermic by 294.3 kJ/mol, compared to 293.7 kJ/mol reported by Raghavachari et al.<sup>10</sup> and 320.1 kJ/mol by Su and Gordon.<sup>11</sup>

Apart from the previously reported reaction channel leading to silanol formation, Figure 1 highlights two new reaction pathways from the intermediate complex **4** that lead to the formation of both *syn*- and *anti*-hydroxysilylene, **9** and **10**, respectively, via H<sub>2</sub> elimination. The net activation energies for these two channels are calculated to be very similar to that for the formation of silanol, being 38.3 kJ/mol for the “*syn*” channel and 36.9 kJ/mol for the “*anti*” channel. The formation of *syn*- and *anti*-hydroxysilylene are predicted to be 111.3 and 112.1 kJ/mol exothermic, respectively. Zachariah and Tsang<sup>1</sup> have previously identified a reaction channel that leads to the formation of *anti*-hydroxysilylene. However, this channel involves a 1,2 hydrogen shift from “*hot*” silanol, rather than originating from intermediate complex **4**. Zachariah and Tsang predict that the activation energy for the conversion of silanol **8** to *anti*-hydroxysilylene **10** is 274 kJ/mol and H<sub>2</sub> elimination is therefore only important at moderate-to-high reaction temperatures (greater than 600 K).<sup>1</sup> Conversely, our much lower activation energies for the “*syn*” and “*anti*” reaction channels from intermediate complex **4** (91.6 and 90.2 kJ/mol, respectively) suggest that H<sub>2</sub> elimination may be an important reaction channel at much lower reaction temperatures.

To gain some insight into the relative propensity for the formation of silanol versus the formation of the two isomers of hydroxysilylene via intermediate complex **4**, we have used Activated Complex Theory (ACT)<sup>28</sup> (or Transition State Theory (TST)<sup>29,30</sup>) to estimate both the preexponential “A-factor” and reaction rate constants for each channel. ACT predicts a reaction rate constant by the expression

$$k(T) = \frac{k_b T}{h} \frac{Q^\ddagger}{Q_{\text{rct}}} \exp\left(\frac{-E_a}{k_b T}\right) \quad (1)$$

where  $k(T)$  is the predicted reaction rate constant,  $Q^\ddagger$  is the

**TABLE 4: Preexponential A-Factors and Reaction Rate Constants  $k$  Calculated for the Silylene-plus-Water System Using Activated Complex Theory<sup>a</sup>**

reaction channel	298.15 K		600 K	
	A-factor (L mol <sup>-1</sup> s <sup>-1</sup> )	$k$ (L mol <sup>-1</sup> s <sup>-1</sup> )	A-factor (L mol <sup>-1</sup> s <sup>-1</sup> )	$k$ (L mol <sup>-1</sup> s <sup>-1</sup> )
4 → 5 → 8	1.58 × 10 <sup>39</sup>	1.31 × 10 <sup>23</sup>	1.78 × 10 <sup>39</sup>	1.82 × 10 <sup>31</sup>
4 → 6 → 9	1.31 × 10 <sup>39</sup>	1.16 × 10 <sup>23</sup>	1.11 × 10 <sup>39</sup>	1.17 × 10 <sup>31</sup>
4 → 7 → 10	1.26 × 10 <sup>39</sup>	2.02 × 10 <sup>23</sup>	1.02 × 10 <sup>39</sup>	1.45 × 10 <sup>31</sup>

<sup>a</sup> See text for details.

partition function density of the activated complex minus the imaginary vibrational degree of freedom (assumed to correspond to the reaction coordinate),  $Q_{\text{act}}$  is the partition function density of the “reactant” (in this case, intermediate complex **4**),  $E_a$  is the activation energy,  $k_b$  is the Boltzmann constant, and the remaining physical constants have their usual meanings. Alexander et al.<sup>16</sup> have measured an inverse temperature dependence for the removal rate constants of singlet silylene and germylene with H<sub>2</sub>O and related compounds, suggesting that the depth of the energy well for the intermediate complex plays an important role in these reaction systems, particularly at lower temperatures. It is therefore reasonable to base the ACT analysis on treating the intermediate complex as the “reactant” due to the fact that many reaction partners become trapped in the initial potential energy well. We have calculated the preexponential factors and reaction rate constants for each of the three reaction channels of interest, viz. **4** → **5** → **8**, **4** → **6** → **9**, and **4** → **7** → **10**, at 298.15 and 600 K. Results of this analysis are presented in Table 4.

The molecular geometries of transition states **5**, **6**, and **7** are all relatively similar, and it is not too surprising, therefore, to see little variation in the predicted values of the preexponential A-factors for each reaction channel. It is therefore unreasonable to conclude that the silanol-forming reaction channel (**4** → **5** → **8**) has a favorable “entropy of reaction” compared to the two newly identified hydroxysilylene-forming channels (**4** → **6** → **9** and **4** → **7** → **10**). Indeed, with each reaction channel exhibiting similar A-factors and activation energies, the predicted rate constants (Table 4) are also very similar. The fact that reaction channel **4** → **7** → **10** (having the lowest activation energy) is predicted to be approximately 80% faster than the other two at room temperature, reducing to ~30% faster at 600 K, further suggests that each reaction channel is equally likely to be accessed as the temperature is increased. In Figure 2 we present the ACT-predicted reaction rate constants for each reaction channel as a function of inverse temperature from 100 to 1500 K. It is clearly evident that all reaction channels have an equal propensity over this wide temperature range. The fact that the plots of the logarithm of  $k$  against reciprocal temperature are linear indicates a much stronger temperature dependence of the exponential term in eq 1 than of the preexponential terms. Hence, the heights of the reaction barriers will control the reaction kinetics rather than the relative “tightness” of each transition state.

**3.2. SiH<sub>2</sub> + MeOH.** The silylene-plus-methanol reaction potential energy surface has been investigated at the MP2/6-311++G(d,p) level of theory. A pictorial summary of the reaction profiles determined from this investigation is presented in Figure 3. In Table 5 we report the point group symmetry of each geometry-optimized stationary point, as well as the total energy, scaled zero-point energy, Hessian index and selected geometric parameters for each stationary point. The relative energies, including scaled zero-point energies, for stationary points on the silylene-plus-methanol system are included in

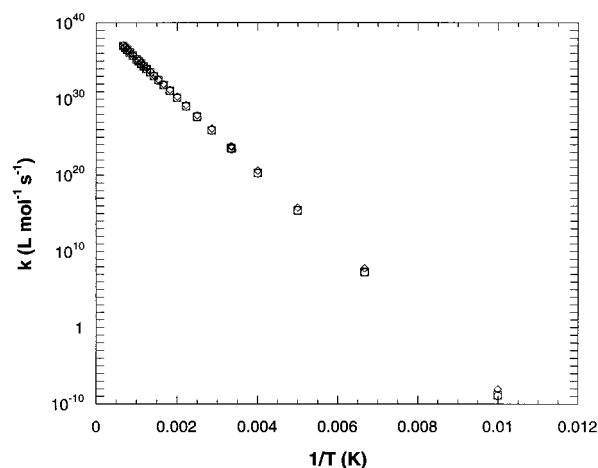
**Figure 2.** ACT-predicted reaction rate constants for each reaction channel (○: **4** → **5** → **8**), (◻: **4** → **6** → **9**), and (△: **4** → **7** → **10**) as a function of inverse temperature from 100 to 1500 K.

Table 6. Complete geometric and vibrational frequency data are available as Supporting Information.<sup>27</sup>

Overall, the appearance of the silylene-plus-methanol reaction potential energy surface is very similar to that for the silylene-plus-water system. The channel involving a 1,2 hydrogen shift has been previously reported by Lee and Boo<sup>15</sup> while the “hydrogen elimination” channels are reported here for the first time. On the basis of the overall similarity in appearance of the silylene-plus-methanol and the silylene-plus-water potential energy surfaces, we expect that each of the three reaction channels via transition states **12**, **13**, and **14** will have similar propensities.

Methyl substitution has increased the well depth of the intermediate complex from 53.3 kJ/mol to 75.8 kJ/mol (see Table 6). The binding energy of 75.8 kJ/mol calculated here for the association complex compares favorably to those reported by Lee and Boo<sup>15</sup> of 88.3 kJ/mol (MP2/6-31G\*) and 83.3 kJ/mol (MP4/6-311G(2df,p)//MP2/6-31G\*). Methyl substitution has decreased the barrier heights (relative to reactants) leading to product formation, from ~38 kJ/mol for reaction with water, to ~14 kJ/mol (Table 6). Lee and Boo predict a much lower barrier to reaction along the 1,2 hydrogen shift reaction channel of 2.5 kJ/mol at the MP4/6-311G(2df,p)//MP2/6-31G\* level of theory, with a zero-point correction determined at the HF/6-31G\* level.<sup>15</sup> Even more striking is their prediction of a barrierless channel, with a transition state energy of -2.1 kJ/mol, when the lower-level zero-point correction term is not included.

In the previous section we identified trends in the predicted energies of stationary points on the silylene-plus-water potential energy surface as a function of the level of theory employed. In particular, we showed that reasonable estimates of well depths and reaction barriers for higher levels of theory can be made, if necessary, by simply adding or subtracting (as appropriate) 2–7 kJ/mol to our reported MP2 results. We believe that a similar scaling process can be made in the silylene-plus-methanol system due to the overall similarity of the two potential energy surfaces. However, some difficulty remains in comparing the silylene-plus-methanol results of this investigation with those reported earlier by Lee and Boo<sup>15</sup> due to the different triple- $\zeta$  basis sets used in each study. In particular, it is not readily apparent what influence the inclusion of diffuse functions (as used here) may have on reported energies compared to the

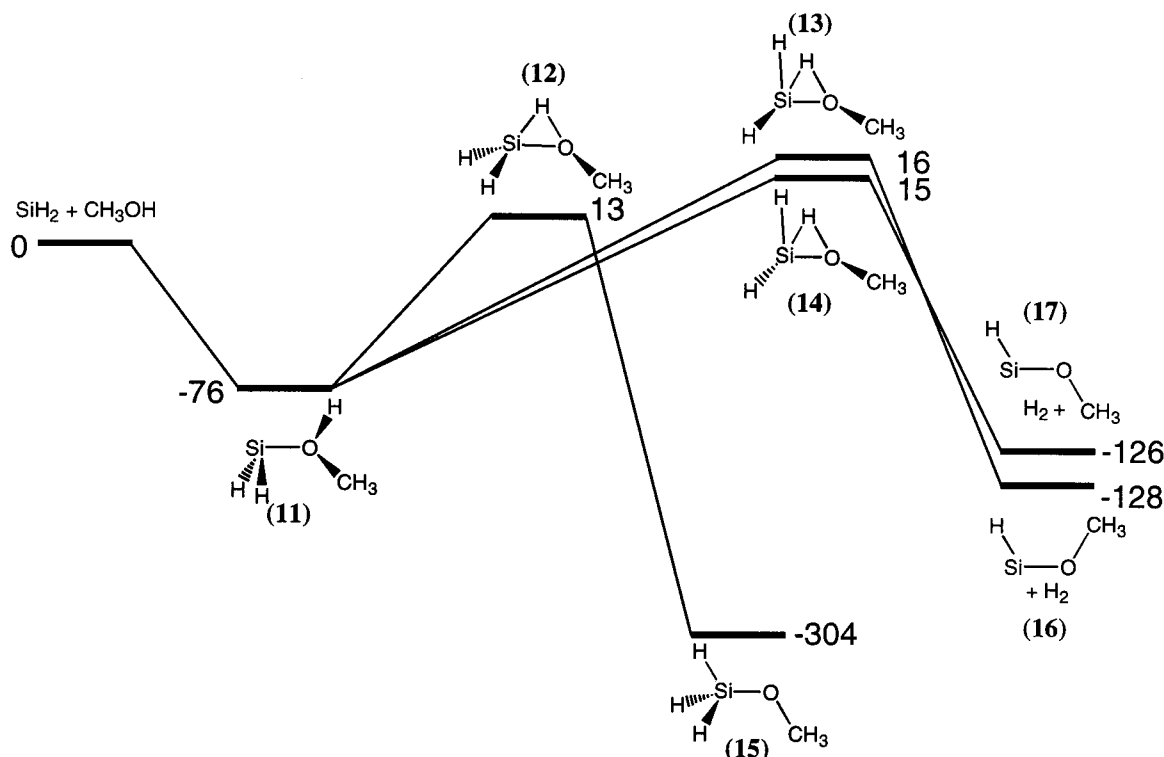
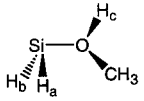
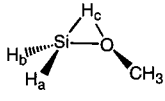
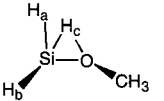
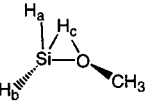
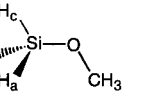
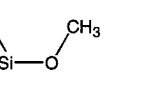
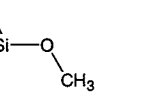


Figure 3. MP2/6-311++G(d,p) stationary points determined on the silylene-plus-methanol reaction potential energy surface.

TABLE 5: The MP2/6-311++G(d,p) Molecular Point Group Symmetry, Total Energy, Scaled Zero-Point Energy (ZPE), Hessian Index, and Selected Geometric Parameters for Each Stationary Point on the Silylene-plus-Methanol Reaction Potential Energy Surface<sup>a</sup>

									
	C <sub>1</sub> (11)	C <sub>1</sub> (12)	C <sub>1</sub> (13)	C <sub>1</sub> (14)	C <sub>s</sub> (15)	C <sub>s</sub> (16)	C <sub>s</sub> (17)		
	total energy	ZPE	Hessian Index	<i>r</i> (Si–O)	<i>r</i> (O–H <sub>c</sub> )	<i>r</i> (Si–H <sub>c</sub> )	∠(Si–O–C)	∠(Si–O–H <sub>c</sub> )	∠(H <sub>a</sub> –Si–H <sub>b</sub> )
reactants (SiH <sub>2</sub> + MeOH)	–405.55684	151.0	0		0.96				92.5
intermediate complex(11)	–405.59095	164.8	0	2.04	0.96	2.55	121.0	111.3	94.2
transition state (12)	–405.55238	151.8	1	1.92	1.26	1.62	115.2	56.8	104.7
transition state (13)	–405.55117	152.3	1	1.88	1.31	1.75	120.2	63.6	87.5
transition state (14)	–405.55198	153.1	1	1.89	1.31	1.75	114.9	63.2	88.7
methoxysilane (15)	–405.67645	161.0	0	1.66	2.51	1.47	121.1	34.1	108.0
<i>syn</i> -methoxysilylene (16)	–404.44173	117.4	0	1.66			129.6		
<i>anti</i> -methoxysilylene (17)	–404.44087	117.8	0	1.67			122.2		
hydrogen (H <sub>2</sub> )	–1.160301	24.2	0						

<sup>a</sup> Total Energies are in Hartrees. ZPEs are in kJ/mol. Distances are in angstroms. Angles are in degrees. Geometric parameters not listed have no meaning in the atom labeling scheme employed.

inclusion of additional polarization functions, particularly the set of higher angular momentum *f* functions as used by Lee and Boo.<sup>15</sup>

To explore the effect of basis set flexibility on reported stationary point energies, we have reoptimized each stationary point found on the MP2/6-311++G(d,p) potential energy surface using a series of increasingly flexible triple-split basis sets, viz., 6-311G(d,p), 6-311G(2d,p), 6-311G(2df,p), 6-311++G(d,p), 6-311++G(2d,p) and 6-311++G(2df,p). The values of the primitive Gaussian exponents and coefficients for all polarization and diffuse functions are the defaults used within the Gaussian 98 program.<sup>18</sup> All optimizations were performed at the MP2 level of theory and the results for each basis set, summarized as the relative energy (in kJ/mol) of each stationary point on the silylene-plus-methanol reaction surface, are reported in Table 7.

Careful inspection of the data in Table 7 highlights a number of general trends in how stationary point energies vary as a function of basis set flexibility. For example, adding a set of diffuse functions to all atoms in a triple- $\zeta$  basis set containing a given complement of polarization functions (e.g., comparing 6-311++G(d,p) to 6-311G(d,p)) has the effect of *raising* all stationary point energies by 5–10 kJ/mol. By comparison, irrespective of whether diffuse functions have been included or not, adding an additional set of *d* and a set of *f* polarization functions to the basis sets already containing one set of *d* functions on the non-hydrogens (and one set of *p* functions on the hydrogen atoms) has the effect of *lowering* all stationary point energies by 15–25 kJ/mol, with the additional set of *f* functions contributing roughly 50% to the energy lowering. The exceptions to this second trend are the initial association complex (structure 11) basis set-dependent relative energies,

**TABLE 6: Comparison of the MP2/6-311++G(d,p) Relative Energies, Including Scaled Zero-Point Energies, of Stationary Points on the Silylene-plus-Methanol, -Ethanol, and -Trifluoromethanol Reaction Potential Energy Surfaces<sup>a</sup>**

	$\Delta E(\text{MP2})$
silylene-plus-methanol	
intermediate Complex (11)	-75.8
transition state (12)	12.5
transition state (13)	16.1
transition state (14)	14.9
methoxysilane (15)	-304.1
<i>syn</i> -methoxysilylene (16) + hydrogen	-128.1
<i>anti</i> -methoxysilylene (17) + hydrogen	-125.5
silylene-plus-ethanol	
intermediate complex (18)	-78.6
transition state (19)	8.9
transition state (20)	12.8
transition state (21)	11.4
ethoxysilane (22)	-306.0
<i>syn</i> -ethoxysilylene (23) + hydrogen	-131.0
<i>anti</i> -Ethoxysilylene (24) + hydrogen	-128.7
silylene-plus-trifluoromethanol	
intermediate complex (25)	-27.7
transition state (26)	39.0
transition state (27)	29.2
transition state (28)	28.4

<sup>a</sup> All values are reported in kJ/mol.

where smaller energy differences are noted as the number of polarization functions is increased.

The data presented in Table 7 also highlight that the prediction of barrierless reaction channels (relative to reactants) by Lee and Boo appears to be a direct consequence of including additional polarization functions in the 6-311G family of basis sets. We predict barrierless reaction channels when the 6-311G-(2d,p), 6-311G(2df,p) and 6-311++G(2df,p) basis sets are used to model the silylene-plus-methanol reaction. The results suggest that irrespective of whether diffuse functions are included in calculations, predicted reaction barriers may be slightly overestimated using basis sets that include only the (d,p) set of polarization functions. However, barriers may well be underestimated if too many polarization functions, for example the (2df,p) set of functions, are included. As we will discuss below, experimental determination of the activation energy for reaction to form products **15**, **16**, and **17** is required to resolve the issue of basis set-dependent predictions of reaction energy barriers.

Completing a comparison of the relative energies reported by Lee and Boo<sup>15</sup> we are able to ascribe their report of a lower MP4/6-311G(2df,p)/MP2/6-31G\* association complex energy of 83.3 kJ/mol to the effect of having additional polarization functions in the single-point energy correction. Additionally, the much lower energy barrier to the 1,2 hydrogen shift channel reported by Lee and Boo of 2.5 kJ/mol at the MP4/6-311G-(2df,p)/MP2/6-31G\* level, compared to our prediction of 12.5 kJ/mol at the MP2/6-311++G(d,p) level can be ascribed to the

fact that the MP4 calculation raises the barrier height relative to the MP2 value by up to 7 kJ/mol, but that the additional polarization functions together with the lack of diffuse functions lowers the barrier by ~20 kJ/mol.

The silylene-plus-methanol reaction potential energy surface reported here at the MP2/6-311++G(d,p) level of theory, predicts that the reaction barrier for the formation of methoxysilane **15**, via transition state **12** is slightly lower (2–3 kJ/mol) than the corresponding “hydrogen elimination” channels accessed via transition states **13** and **14** (see Table 6). Also, the relative energies of the “syn” and “anti” hydrogen-elimination products **16** and **17** swap compared to their corresponding transition states **13** and **14**. The Si–O bond length in intermediate complex **11** is 2.04 Å, much shorter than the 2.12 Å bond length found in intermediate complex **4**. This is expected because methyl is a better electron donor than hydrogen, allowing for a stronger Si–O bond to form. The formation of a stronger Si–O bond explains the deeper energy well for intermediate complex **11** compared to the analogous intermediate complex **4** on the silylene-plus-water reaction surface. Indeed, the shorter Si–O bond also accounts for the significantly lower energies of the three transition states **12**, **13** and **14**. Overall, the silylene-plus-methanol potential energy surface exhibits lower activation barriers for product formation relative to the reactants. However, any species trapped in the deeper energy well corresponding to intermediate complex **11** will experience a barrier to further reaction of 88 kJ/mol (Table 6), which is similar to the 92 kJ/mol barrier calculated for the silylene-plus-water system. Alexander et al.<sup>16</sup> have concluded that, from the perspective of the intermediate complex, at temperatures below ~450 K “unimolecular dissociation” back to reactants is more likely than further reaction leading to products **15**, **16**, and **17**. However, these workers also note that some evidence exists suggesting that in addition to “unimolecular dissociation” from intermediate complex **11**, an additional reaction channel is operative. Unfortunately, Alexander et al.<sup>16</sup> provide no analysis of their data to estimate the barrier height for this additional reaction channel. Such modeling would be required to compare to the ab initio data presented in Table 7.

**3.3. SiH<sub>2</sub> + EtOH.** A pictorial summary of the reaction profiles determined from our MP2/6-311++G(d,p) investigation into the silylene-plus-ethanol system is presented in Figure 4. In Table 8 we report the point group symmetry of each geometry-optimized stationary point, as well as the total energy, scaled zero-point energy, Hessian index, and selected geometric parameters for each stationary point. The relative energies, including scaled zero-point energies, for stationary points on the silylene-plus-ethanol surface are included in Table 6.

Methyl and ethyl groups have similar electron donating strengths, indicating that substitution of a methyl group for an ethyl group should not significantly alter the electronic environ-

**TABLE 7: Comparison of the Relative Energies of Stationary Points on the Silylene-plus-Methanol Reaction Potential Energy Surface for Several Triple-Split Basis Sets<sup>a</sup>**

basis set	reactants	(11)	(12)	(13)	(14)	(15)	(16) + H <sub>2</sub>	(17) + H <sub>2</sub>
6-311G(d,p)	0.0	-95.1	7.1	7.5	6.7	-321.4	-122.3	-118.3
6-311G(2d,p)	0.0	-96.2	-2.5	-3.5	-5.0	-337.7	-138.1	-134.8
6-311G(2df,p)	0.0	-102.7	-11.9	-12.6	-14.0	-347.0	-146.9	-143.2
6-311++G(d,p)	0.0	-89.6	11.7	14.9	12.8	-314.0	-118.6	-116.4
6-311++G(2d,p)	0.0	-86.1	5.2	6.2	3.7	-327.6	-129.4	-128.0
6-311++G(2df,p)	0.0	-92.1	-4.1	-2.6	-5.2	-337.3	-138.3	-136.6

<sup>a</sup> All reported energies are determined from geometry optimizations at the MP2 level of theory. No corrections for zero-point effects have been included, hence the values reported here for the 6-311++G(d,p) basis set differ from those reported in Table 6 where scaled zero-point energy contributions have been included. Energies are reported in kJ/mol. See text for details.

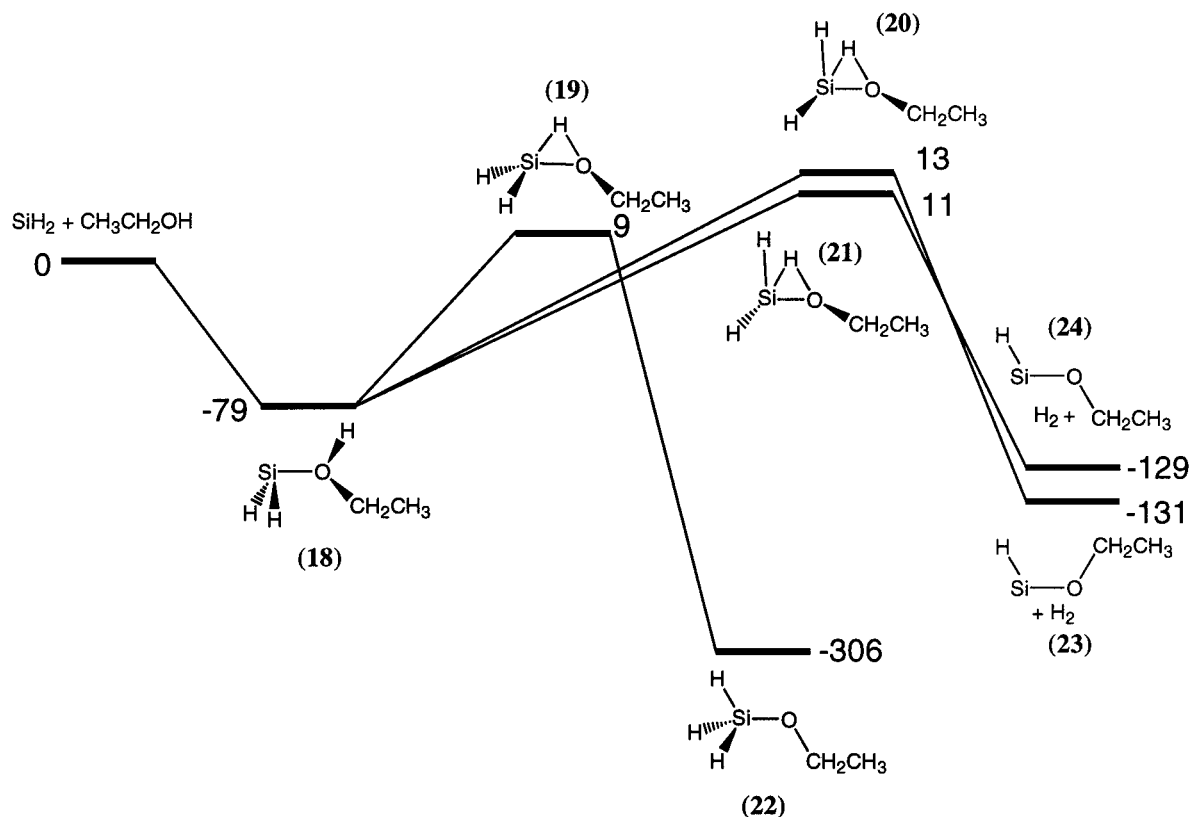


Figure 4. MP2/6-311++G(d,p) stationary points determined on the silylene-plus-ethanol reaction potential energy surface.

TABLE 8: The MP2/6-311++G(d,p) Molecular Point Group Symmetry, Total Energy, Scaled Zero-Point Energy (ZPE), Hessian Index and Selected Geometric Parameters for Each Stationary Point on the Silylene-plus-Ethanol Reaction Potential Energy Surface<sup>a</sup>

	C <sub>1</sub> (18)	C <sub>1</sub> (19)	C <sub>1</sub> (20)	C <sub>1</sub> (21)	C <sub>1</sub> (22)	C <sub>1</sub> (23)	C <sub>1</sub> (24)		
	total energy	ZPE	Hessian index	r(Si-O)	r(O-H <sub>c</sub> )	r(Si-H <sub>c</sub> )	∠(Si-O-C <sub>d</sub> )	∠(Si-O-H <sub>c</sub> )	∠(H <sub>a</sub> -Si-H <sub>b</sub> )
reactants (SiH <sub>2</sub> + EtOH)	-444.75719	218.4	0		0.96				92.5
intermediate complex (18)	-444.79243	232.3	0	2.03	0.97	2.55	121.4	111.5	94.3
transition state (19)	-444.75413	219.3	1	1.92	1.26	1.62	114.9	56.7	104.7
transition state (20)	-444.75282	219.7	1	1.89	1.31	1.75	119.8	63.3	87.4
transition state (21)	-444.75374	220.7	1	1.89	1.31	1.74	114.7	63.0	88.6
ethoxysilane (22)	-444.87768	228.7	0	1.66	2.52	1.47	121.2	34.1	108.0
<i>syn</i> -ethoxysilylene (23)	-443.643398	185.3	0	1.66			129.4		
<i>anti</i> -ethoxysilylene (24)	-443.642663	185.7	0	1.67			122.1		
hydrogen (H <sub>2</sub> )	-1.160301	24.2	0						

<sup>a</sup> Total energies are in hartrees. ZPEs are in kJ/mol. Distances are in angstroms. Angles are in degrees. Geometric parameters not listed have no meaning in the atom labeling scheme employed.

ment experienced by the oxygen atom. Inspections of Figures 3 and 4 shows that the energetics of the reaction potential energy surfaces are almost identical. For silylene-plus-ethanol, we predict a marginal *decrease* of 3–4 kJ/mol in the transition state barrier heights and a similar *increase* in the well depth of intermediate complex 18, relative to the silylene-plus-methanol system. We expect that the reaction kinetics for these two reaction systems will be very similar.

In the silylene-plus-water system, each reaction product (structures 8, 9, and 10) is predicted to possess C<sub>s</sub> molecular symmetry. A similar situation exists for the silylene-plus-methanol reaction system, with products 15, 16, and 17 possessing C<sub>s</sub> symmetry. However it is interesting to note that in the silylene-plus-ethanol system, all three reaction products (structures 22, 23, and 24) possess C<sub>1</sub> symmetry, with the

terminal methyl group bent out of what would be the C<sub>s</sub> symmetry plane. Furthermore, the C<sub>s</sub> configurations of all three products are transition states on the MP2 surfaces, linking degenerate minima of C<sub>1</sub> symmetry via an out-of-plane methyl wag.

**3.4. SiH<sub>2</sub> + CF<sub>3</sub>OH.** To explore the influence of the electronic environment around the central oxygen atom on reactivity with silylene, the alkyl substituents were replaced by a strong electron-withdrawing trifluoromethyl group, yielding trifluoromethanol as the reaction partner. For this reaction system, investigations were limited to determining the relative energies of the intermediate complexes and transition states. In Table 9 we report the point group symmetry of each geometry-optimized stationary point, as well as the total energy, scaled zero-point energy, Hessian index and selected geometric



**TABLE 9: MP2/6-311++G(d,p) Molecular Point Group Symmetry, Total Energy, Scaled Zero-Point Energy (ZPE), Hessian Index, and Selected Geometric Parameters for Each Stationary Point on the Silylene-plus-Trifluoromethanol Reaction Potential Energy Surface<sup>a</sup>**

	total energy	ZPE	Hessian index	$r(\text{Si}-\text{O})$	$r(\text{O}-\text{H}_c)$	$r(\text{Si}-\text{H}_c)$	$\angle(\text{Si}-\text{O}-\text{C}_d)$	$\angle(\text{Si}-\text{O}-\text{H}_c)$	$\angle(\text{H}_a-\text{Si}-\text{H}_b)$
reactants ( $\text{SiH}_2 + \text{CF}_3\text{OH}$ )	-702.83860	97.5	0		0.96				92.5
intermediate complex ( <b>25</b> )	-702.85264	106.6	0	2.30	0.97	2.78	125.2	109.6	93.4
transition state ( <b>26</b> )	-702.82304	95.6	1	2.08	1.22	1.67	123.2	53.1	104.3
transition state ( <b>27</b> )	-702.82774	98.2	1	2.04	1.23	1.81	123.9	61.6	88.3
transition state ( <b>28</b> )	-702.82814	98.4	1	2.04	1.23	1.81	121.1	61.3	88.9

<sup>a</sup> Total energies are in hartrees. ZPEs are in kJ/mol. Distances are in angstroms. Angles are in degrees. Geometric parameters not listed have no meaning in the atom labeling scheme employed.

**TABLE 10: MP2/6-311++G(d,p) Molecular Point Group Symmetry, Total Energy, Scaled Zero-Point Energy (ZPE), Hessian Index, and Selected Geometric Parameters for Each Stationary Point on the Germylene-plus-Water Reaction Potential Energy Surface<sup>a</sup>**

	total energy	ZPE	Hessian index	$r(\text{Ge}-\text{O})$	$r(\text{O}-\text{H}_c)$	$r(\text{Ge}-\text{H}_c)$	$\angle(\text{Ge}-\text{O}-\text{H}_d)$	$\angle(\text{Ge}-\text{O}-\text{H}_c)$	$\angle(\text{H}_a-\text{Ge}-\text{H}_b)$
reactants ( $\text{GeH}_2 + \text{H}_2\text{O}$ )	-2152.79566	77.5	0		0.96				91.8
intermediate complex ( <b>29</b> )	-2152.81814	90.4	0	2.27	0.96	2.84	117.0	117.2	94.0
transition state ( <b>30</b> )	-2152.76395	78.6	1	2.07	1.38	1.63	108.4	51.5	105.5
transition state ( <b>31</b> )	-2152.77555	81.2	1	2.03	1.35	1.86	116.6	62.9	87.6
transition state ( <b>32</b> )	-2152.77580	81.8	1	2.03	1.34	1.86	114.1	63.0	88.4
germinol ( <b>33</b> )	-2152.86448	87.1	0	1.80	2.62	1.52	116.9	34.1	109.6
<i>syn</i> -hydroxygermylene ( <b>34</b> )	-2151.65923	46.7	0	1.82			114.1		
<i>anti</i> -hydroxygermylene ( <b>35</b> )	-2151.65946	47.4	0	1.82			110.7		
hydrogen ( $\text{H}_2$ )	-1.16030	24.2	0						

<sup>a</sup> Total energies are in hartrees. ZPEs are in kJ/mol. Distances are in angstroms. Angles are in degrees. Geometric parameters not listed have no meaning in the atom labeling scheme employed.

parameters for each stationary point. The relative energies, including scaled zero-point energies, for all stationary points are included in Table 6.

We would expect that the electron withdrawing nature of trifluoromethanol to influence the energetics of the silylene-plus-trifluoromethanol reaction potential energy surface in quite a different way to the silylene-plus-methanol and silylene-plus-ethanol surfaces. Indeed, with the reduced electron density available for the Si-O bond formed between  $\text{SiH}_2$  and  $\text{CF}_3\text{OH}$  being a primary factor governing the overall reaction potential energy surface, we would expect reaction energetics similar to those predicted for the silylene-plus-water reaction system.

The silylene-plus-trifluoromethanol reaction surface features the most weakly bound intermediate complex (structure **25**) with a well depth of only 27.7 kJ/mol; the Si-O bond length in intermediate complex **25** is unusually long at 2.30 Å. These predictions are entirely consistent with less electron density being available within the critical Si-O bond. The longer Si-O bond in association complex **25** would also be expected to result in larger activation barriers for both the H atom migration and  $\text{H}_2$  elimination reaction channels. The 1,2 hydrogen shift barrier is predicted to be 39.0 kJ/mol, compared to 38.5 kJ/mol with water as the reaction partner. However, the energy barriers to  $\text{H}_2$  elimination are lower than in the case of reacting with water.

For hydrogen elimination, the “syn” channel barrier is 29.2 kJ/mol, compared to 38.3 kJ/mol with water, while the “anti” barrier is 28.4 kJ/mol compared to 36.9 kJ/mol with water.

**3.5.  $\text{GeH}_2 + \text{H}_2\text{O}$ .** A summary of the reaction energetics from our MP2/6-311++G(d,p) investigation into the germylene-plus-water reaction system is presented in Table 10. We report the point group symmetry of each geometry-optimized stationary point, as well as the total energy, scaled zero-point energy, Hessian index and selected geometric parameters for each stationary point. The relative energies, including scaled zero-point energies, for stationary points on the germylene-plus-water surface are included in Table 11.

The germylene oxidation chemistry is qualitatively similar to that of silylene, with the possibility of both H atom migration and  $\text{H}_2$  elimination processes being active. All energy barriers to reaction are higher, and reaction exothermicities are smaller. However, the  $\text{H}_2$  elimination processes are predicted to occur in preference to the germinol-forming migration channel. Compared to the silylene-plus-water system, the germylene reaction potential energy surface exhibits a barrier to reaction involving a 1,2 hydrogen shift that is very large. The energy barrier is 84.4 kJ/mol with respect to the reactants and 130.5 kJ/mol from the intermediate complex energy well. The higher energy barrier to H atom migration is not unexpected due to

**TABLE 11: Comparison of the MP2/6-311++G(d,p) Relative Energies, Including Scaled Zero-Point Energies, of Stationary Points on the Germylene-plus-Water, and -Methanol Reaction Potential Energy Surfaces<sup>a</sup>**

	$\Delta E(\text{MP2})$
germylene-plus-water	
intermediate complex (29)	-46.1
transition state (30)	84.4
transition state (31)	56.5
transition state (32)	56.4
germinol (33)	-171.1
<i>syn</i> -hydroxygermylene (34) + hydrogen	-69.8
<i>anti</i> -hydroxygermylene (35) + hydrogen	-69.2
germylene-plus-methanol	
intermediate complex (36)	-63.1
transition state (37)	63.4
transition state (38)	37.8
transition state (39)	38.0
methoxygermane (40)	-179.2
<i>syn</i> -methoxygermylene (41) + hydrogen	-81.8
<i>anti</i> -methoxygermylene (42) + hydrogen	-79.5

<sup>a</sup> All values are reported in kJ/mol.

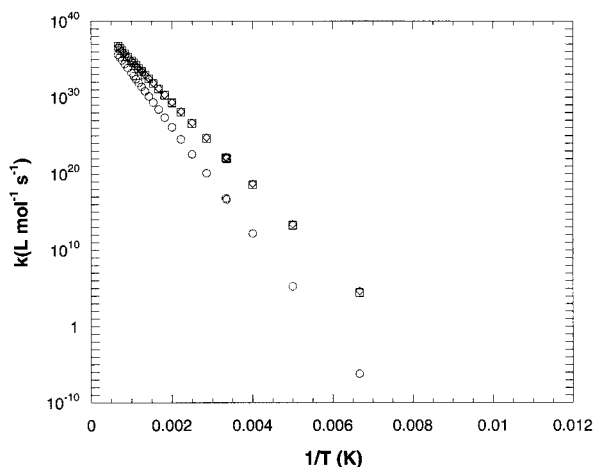


**Figure 5.** ACT-predicted reaction rate constants for each reaction channel (O: 29 → 30 → 33), (□: 29 → 31 → 34) and (Δ: 29 → 32 → 35) as a function of inverse temperature from 100 to 1500 K.

the larger size of the germanium atom. Indeed, the larger germanium atom size favors the “hydrogen elimination” channels by nearly 30 kJ/mol.

The temperature-dependent reaction rate constants predicted from a simple ACT analysis using the germylene-plus-water reaction potential energy surface are presented in Figure 5. As for the data presented in Figure 2, the predicted rate constants are calculated in each case assuming the “reactant” to be the intermediate association complex. The ACT analysis predicts that at room temperature the H<sub>2</sub> elimination channels have reaction rate constants approximately 5 orders of magnitude faster than for the 1,2 hydrogen shift channel. Clearly hydrogen elimination is the dominant reaction channel in the oxidation chemistry of germylene at low-to-moderate temperatures. As with the equivalent silylene reactions, the linearity of the temperature-dependent rate constant plots in Figure 5 indicates that the reaction barrier heights dominate the kinetics rather than any entropic effects attributable to transition state geometries.

**3.6. GeH<sub>2</sub> + MeOH.** A summary of the reaction energetics from our MP2/6-311++G(d,p) investigation into the germylene-plus-methanol reaction system is presented in Table 12. We report the point group symmetry of each geometry-optimized stationary point, as well as the total energy, scaled zero-point energy, Hessian index, and selected geometric parameters for

each stationary point. The relative energies, including scaled zero-point energies, for stationary points on the germylene-plus-water surface are included in Table 11.

Compared to the analogous silylene system, the germylene-plus-methanol reaction potential energy surface shows overall significantly higher barriers to reaction, but is otherwise qualitatively quite similar. Again there exists a strong (~25 kJ/mol) energetic preference for the H<sub>2</sub> elimination channels compared to the H atom migration process. Furthermore, the reaction exothermicities are again predicted to be much lower than for the equivalent silylene reactions.

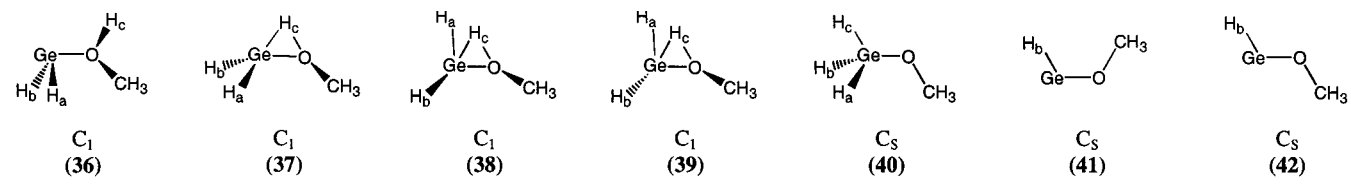
A comparison of the germylene-plus-water and germylene-plus-methanol reaction potential energy surfaces shows that the greater electron donating ability of the methyl substituent lowers all transition state energy barriers and the intermediate complex well depth by ~20 kJ/mol. This behavior is similar to that predicted for the analogous silicon reaction systems. Drawing upon the concepts of ACT discussed earlier, the similarities in the molecular geometries of each transition state makes it unlikely that the H<sub>2</sub> elimination channels are entropically unfavored. Therefore, with the significantly lower barriers to reaction, we expect that H<sub>2</sub>-elimination will again constitute the dominant reaction channels.

**3.7. SiH<sub>2</sub> + MeOMe and GeH<sub>2</sub> + MeOMe.** Alexander and co-workers have measured the removal rate constants for the reactions of silylene and germylene with dimethyl ether.<sup>16</sup> These workers have found that compared to methanol and water, the dimethyl ether removal rate constants are significantly larger, suggesting that different chemical pathways may be operative for these systems. Certainly, there is no obvious avenue for H atom migration or H<sub>2</sub> elimination with dimethyl ether as the reaction partner.

A summary of the reaction energetics from our MP2/6-311++G(d,p) investigation into the silylene-plus-dimethyl ether and germylene-plus-dimethyl ether reaction systems is presented in Table 13. We report the point group symmetry of each geometry-optimized stationary point, as well as the total energy, scaled zero-point energy, Hessian index, and selected geometric parameters for each stationary point. The relative energies, including scaled zero-point energies, for stationary points on both potential energy surfaces are also included in Table 13.

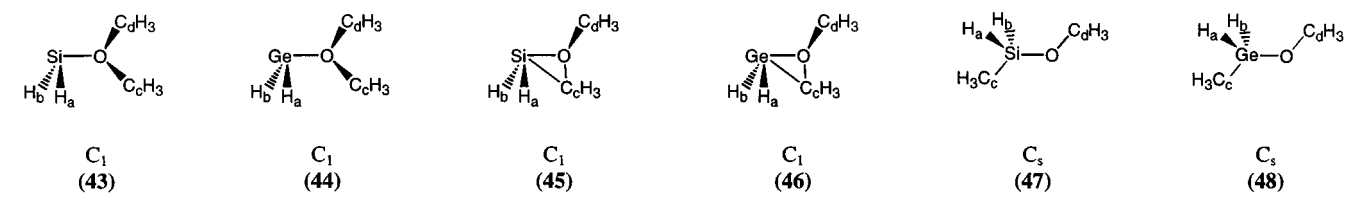
The silylene-plus-dimethyl ether and germylene-plus-dimethyl ether reaction potential energy surfaces each display similar characteristics, with relatively deep energy wells for the initially formed association complexes. However, compared to all previous reactions discussed, no reaction channels have been found that correspond either to H atom migration from the oxygen atom to the group IV element or to H<sub>2</sub> elimination. Rather, a relatively high-energy channel that corresponds to the migration of an entire methyl group from the oxygen atom to the group IV element has been identified. The methyl group migration differs from the previously reported H atom migration channels in that it proceeds “syn” to the silylene (germylene) hydrogen atoms. The geometries of transition states 45 and 46 are similar to those reported by Lee and Boo in their study of the insertion of silylene into the C–O bond of methanol.<sup>15</sup>

The energy barriers to the methyl-migration reactions leading to the formation of the highly exothermic products methoxymethylsilane 47 and methoxymethylgermane 48 are quite large, being 193.3 and 229.1 kJ/mol, respectively. The overall reaction exothermicities are 365.1 kJ/mol for the formation of product 47 and 230.9 kJ/mol for the formation of product 48. Intrinsic reaction coordinate calculations from transition states 45 and 46 confirm that final product formation involves an inversion

**TABLE 12: The MP2/6-311++G(d,p) Molecular Point Group Symmetry, Total Energy, Scaled Zero-point Energy (ZPE), Hessian Index, and Selected Geometric Parameters for Each Stationary Point on the Germylene-plus-Methanol Potential Energy Surface<sup>a</sup>**


	total energy	ZPE	Hessian index	$r(\text{Ge}-\text{O})$	$r(\text{O}-\text{H}_c)$	$r(\text{Ge}-\text{H}_c)$	$\angle(\text{Ge}-\text{O}-\text{C})$	$\angle(\text{Ge}-\text{O}-\text{H}_c)$	$\angle(\text{H}_a-\text{Ge}-\text{H}_b)$
reactants ( $\text{GeH}_2 + \text{MeOH}$ )	-2191.96596	149.0	0		0.96				91.8
intermediate complex (36)	-2191.99442	160.6	0	2.21	0.96	2.70	119.6	110.4	92.5
transition state (37)	-2191.94128	147.6	1	2.05	1.38	1.62	112.7	52.2	105.8
transition state (38)	-2191.95145	148.7	1	2.02	1.35	1.87	118.3	63.8	86.3
transition state (39)	-2191.95154	149.1	1	2.03	1.36	1.86	113.5	63.2	87.3
methoxygermane (40)	-2192.03650	155.0	0	1.80	2.65	1.53	117.3	33.8	109.6
syn-methoxygermylene (41)	-2190.83292	114.6	0	1.80			126.7		
anti-methoxygermylene (42)	-2190.83216	114.9	0	1.81			120.2		
hydrogen ( $\text{H}_2$ )	-1.16030	24.2	0						

<sup>a</sup> Total Energies are in hartrees. ZPEs are in kJ/mol. Distances are in angstroms. Angles are in degrees. Geometric parameters not listed have no meaning in the atom labeling scheme employed.

**TABLE 13: MP2/6-311++G(d,p) Molecular Point Group Symmetry, Total Energy, Scaled Zero-point Energy (ZPE), Relative Energies, Hessian Index, and Selected Geometric Parameters (the symbol X represents Si or Ge) for Each Stationary Point on the Silylene-plus-Dimethyl Ether and Germylene-plus-Dimethyl Ether Reaction Potential Energy Surfaces<sup>a</sup>**


	total energy	ZPE	$\Delta E(\text{MP2})$	Hessian index	$r(\text{X}-\text{O})$	$r(\text{O}-\text{C}_c)$	$r(\text{X}-\text{C}_c)$	$\angle(\text{X}-\text{O}-\text{C}_d)$	$\angle(\text{X}-\text{O}-\text{C}_c)$	$\angle(\text{H}_a-\text{X}-\text{H}_b)$
reactants ( $\text{SiH}_2 + \text{CH}_3\text{OCH}_3$ )	-444.73544	218.6	0.0	0		1.41				92.5
intermediate complex (43)	-444.77266	232.0	-84.3	0	2.03	1.44	2.92	117.9	113.6	94.2
transition state (45)	-444.67383	250.1	193.3	1	1.86	1.96	2.53	112.5	82.9	102.3
methyl methoxy-silane (47)	-444.88887	256.3	-365.1	0	1.67	2.84	1.86	121.3	38.7	107.6
reactants ( $\text{GeH}_2 + \text{CH}_3\text{OCH}_3$ )	-2231.14456	216.5	0.0	0		1.41				91.8
intermediate complex (44)	-2231.17556	227.8	-70.4	0	2.20	1.44	3.12	112.5	117.0	92.6
transition state (46)	-2231.06772	243.9	229.1	1	2.00	2.03	2.60	110.2	80.4	100.9
methyl methoxy-germane (48)	-2231.24540	250.4	-230.9	0	1.81	2.98	1.94	117.8	39.0	109.0

<sup>a</sup> Total Energies are in hartrees. ZPEs and  $\Delta E$ 's are in kJ/mol. Distances are in angstroms. Angles are in degrees. Geometric parameters not listed have no meaning in the atom labeling scheme employed.

of the silylene and germylene hydrogen atoms about the silicon and germanium atoms as the migrating methyl group adopts an "anti" configuration with respect to the methoxy methyl group. Both products **47** and **48** possess  $C_s$  molecular symmetry.

The significantly larger energy barriers suggest that formation of products **47** and **48** is unlikely to be a significant reaction channel in either of these systems at other than at very high temperatures. At lower temperatures, the larger removal rate constants measured by Alexander et al.<sup>16</sup> can be attributed to trapping of the initial association complex in the relatively deep energy well. Once trapped in the well, dissociation back to reactants is diminished, the process being manifest as an increase in the reactant removal reaction rates.

#### 4. Conclusions

We have employed ab initio molecular orbital theory to investigate the reaction potential energy surfaces of singlet silylene and singlet germylene with water, methanol, ethanol, dimethyl ether and trifluoromethanol. In addition to the previously reported 1,2 hydrogen shift reaction channel, we have identified new stereospecific "syn" and "anti"  $\text{H}_2$  elimination channels for all reaction systems except for those involving dimethyl ether. The overall appearance of the reaction potential energy surface is qualitatively similar for each reaction family, with all reactions forming an initial association complex involving the empty p atomic-like molecular orbital on the Group XIV element and the electron rich oxygen atom prior to

final product formation. For reactions involving dimethyl ether, migration of an entire methyl group from the ether to the Group XIV element occurs “syn” to the silylene (germylene) hydrogen atoms.

A simple activated complex theory (ACT) analysis has been performed on the calculated silylene-plus-water and germylene-plus-water reaction potential energy surfaces. In the case of silylene-plus-water, the H<sub>2</sub> elimination channels are predicted to have an equal propensity for reaction compared to the H atom migration channel. However, for germylene-plus-water system, we predict that H<sub>2</sub> elimination is significantly more likely to proceed, even at low-to-moderate reaction temperatures.

**Acknowledgment.** This work was supported by the The University of Adelaide. Computing resources provided by the South Australian Centre for Parallel Computing (SACPC) and The South Australian Computational Chemistry Facility (SAC-CF) are gratefully acknowledged. We thank M. R. Hammer for assistance in evaluating the ACT reaction rate constants. We thank W. D. Lawrance and U. N. Alexander (Flinders University) for helpful discussions.

**Supporting Information Available:** A listing of complete geometry specifications (in Cartesian coordinates) for each stationary point on the potential energy surface for each reaction, together with a full listing of unscaled vibrational frequencies. This material is available free of charge via the Internet at <http://pubs.acs.org>.

## References and Notes

- Zachariah, M. R.; Tsang, W. *J. Phys. Chem.* **1995**, *99*, 5308.
- Zachariah, M. R.; Tsang, W. *At. Res. Soc. Symp. Proc.* **1993**, *282*, 493.
- Zachariah, M. R.; Jr., D. R. F. B. *J. Aerosol Sci.* **1994**, *25*, 487 and references therein.
- Lucas, D. J.; Curtiss, L. A.; Pople, J. A. *J. Chem. Phys.* **1993**, *99*, 6697 and references therein.
- Gordon, M. S.; Pederson, L. A. *J. Phys. Chem.* **1990**, *94*, 5527.
- Zachariah, M. R.; Tsang, W. *J. Phys. Chem.* **1995**, *99*, 5308 and references therein.
- Gaspar, P. P. In *Reactive Intermediates*; Jones, M., Moss, R. A., Eds.; Wiley-Interscience: New York, 1978; Vol. 1; p 229.
- Tang, Y. N. In *Reactive Intermediates*; Abramovitch, R. A., Ed.; Plenum Press: New York, 1982; Vol. 2, p 297.
- Su, S.; Gordon, M. S. *Chem. Phys. Lett.* **1993**, *204*, 306 and references therein.
- Raghavachari, K.; Chandrasekhar, J.; Gordon, M. S.; Dykema, K. *J. Am. Chem. Soc.* **1984**, *106*, 5853.
- Su, S.; Gordon, M. S. *Chem. Phys. Lett.* **1993**, *204*, 306.
- Darling, C. L.; Schegel, H. B. *J. Phys. Chem.* **1993**, *97*, 8207.
- Lucas, D. J.; Curtiss, L. A.; Pople, J. A. *J. Chem. Phys.* **1993**, *99*, 6697.
- Curtiss, L. A.; Raghavachari, K.; Trucks, G. W.; Pople, J. A. *J. Chem. Phys.* **1991**, *94*, 7221.
- Lee, S. Y.; Boo, B. H. *J. Mol. Struct.* **1996**, *366*, 79–82.
- Alexander, U. N. Direct Kinetic Studies of Silylene and Germylene. Ph.D. Thesis, The Flinders University of South Australia, 2000.
- Frisch, M. J.; Trucks, G. W.; Schlegel, H. B.; Gill, P. M. W.; Johnson, B. G.; Robb, M. A.; Cheeseman, J. R.; Keith, T.; Petersson, G. A.; Montgomery, J. A.; Raghavachari, K.; Al-Laham, M. A.; Zakrzewski, V. G.; Ortiz, J. V.; Foresman, J. B.; Cioslowski, J.; Stefanov, B. B.; Nanayakkara, A.; Challacombe, M.; Peng, C. Y.; Ayala, P. Y.; Chen, W.; Wong, M. W.; Andres, J. L.; Replogle, E. S.; Gomperts, R.; Martin, R. L.; Fox, D. J.; Binkley, J. S.; Defrees, D. J.; Baker, J.; Stewart, J. P.; Head-Gordon, M.; Gonzalez, C.; Pople, J. A.; *Gaussian 94*, Revision E.2; Gaussian, Inc.: Pittsburgh, PA, 1995.
- Frisch, M. J.; Trucks, G. W.; Schlegel, H. B.; Scuseria, G. E.; Robb, M. A.; Cheeseman, J. R.; Zakrzewski, V. G.; Montgomery, J. A.; Stratmann, R. E.; Burant, J. C.; Dapprich, S.; Millam, J. M.; Daniels, A. D.; Kudin, K. N.; Strain, M. C.; Farkas, O.; Tomasi, J.; Barone, V.; Cossi, M.; Cammi, R.; Mennucci, B.; Pomelli, C.; Adamo, C.; Clifford, S.; Ochterski, J.; Petersson, G. A.; Ayala, P. Y.; Cui, Q.; Morokuma, K.; Malick, D. K.; Rabuck, A. D.; Raghavachari, K.; Foresman, J. B.; Cioslowski, J.; Ortiz, J. V.; Stefanov, B. B.; Liu, G.; Liashenko, A.; Piskorz, P.; Komaromi, I.; Gomperts, R.; Martin, R. L.; Fox, D. J.; Keith, T.; Al-Laham, M. A.; Peng, C. Y.; Nanayakkara, A.; Gonzalez, C.; Challacombe, M.; Gill, P. M. W.; Johnson, B. G.; Chen, W.; Wong, M. W.; Andres, J. L.; Head-Gordon, M.; Replogle, E. S.; Pople, J. A.; *Gaussian 98, Revision A.7*; Gaussian, Inc.: Pittsburgh, PA, 1998.
- The MP4(SDTQ) method involves a fourth-order Møller–Plesset perturbation theory calculation in the space of single, double, triple, and quadruple electron substitutions.
- Krishnan, R.; Frisch, M. J.; Pople, J. A. *J. Chem. Phys.* **1980**, *72*, 4244 and references therein.
- The QCISD(T) theory involves a quadratic configuration interaction calculation incorporating all single and double electron substitutions and a triples contribution to the calculated energy.
- Foresman, J. B.; Frisch, M. J. *Exploring Chemistry with Electronic Structure Methods*, 2nd ed.; Gaussian Inc.: Pittsburgh, PA, 1996.
- A local minimum on a potential energy surface is characterised by having all real vibrational frequencies and all positive eigenvalues in the Hessian matrix while a transition state is characterised by having only one imaginary vibrational frequency and only one negative eigenvalue in the Hessian matrix.
- Curtiss, L. A.; Raghavachari, K.; Trucks, G. W.; Pople, J. A. *J. Chem. Phys.* **1991**, *94*, 7221.
- Gonzalez, C.; Schlegel, H. B. *J. Chem. Phys.* **1989**, *90*, 2154.
- Unless stated otherwise, all energies and geometric parameters reported in the discussion refer to those calculated at the MP2/6-311++G-(d, p) level of theory.
- See Supporting Information Available paragraph above.
- Laidler, K. J. *Theories of Chemical Reaction Rates*; McGraw-Hill: New York, 1969.
- Steinfeld, J. I.; Francisco, J. S.; Hase, W. L.; *Chemical Kinetics and Dynamics*; Prentice Hall: Englewood Cliffs, 1989.
- Gilbert, R. G.; Smith, S. C. *Theory of Unimolecular and Recombination Reactions*; Blackwell Scientific: Oxford, 1990.